

Gravitational Theory, Galaxy Rotation Curves and Cosmology without Dark Matter

J. W. Moffat

*The Perimeter Institute for Theoretical Physics, Waterloo, Ontario, N2J 2W9,
Canada*

and

*Department of Physics, University of Waterloo, Waterloo, Ontario N2Y 2L5,
Canada*

Abstract

Einstein gravity coupled to a massive skew symmetric field $F_{\mu\nu\lambda}$ leads to an acceleration law that modifies the Newtonian law of attraction between particles. We use a framework of non-perturbative renormalization group equations as well as observational input to characterize special renormalization group trajectories to allow for the running of the effective gravitational coupling G and the coupling of the skew field to matter. Strong renormalization effects occur at large and small momentum scales. The latter lead to an increase of Newton's constant at large galactic and cosmological distances. For weak fields a fit to the flat rotation curves of galaxies is obtained in terms of the mass (mass-to-light ratio M/L) of galaxies. The fits assume that the galaxies are not dominated by exotic dark matter and that the effective gravitational constant G runs with distance scale. The equations of motion for test particles yield predictions for the solar system and the binary pulsar PSR 1913+16 that agree with the observations. The gravitational lensing of clusters of galaxies can be explained without exotic dark matter. An FLRW cosmological model with an effective $G = G(t)$ running with time can lead to consistent fits to cosmological data without assuming the existence of exotic cold dark matter.

e-mail: jmoffat@perimeterinstitute.ca

1 Introduction

A nonsymmetric gravity theory (NGT) has been applied to explain rotation curves of galaxies and cosmology, without invoking dominant dark matter and identifying dark energy with the cosmological constant [1, 2, 3, 4]. In the following, we develop a simpler gravitational theory based on Einstein's general relativity (GR) and a

skew symmetric rank three tensor field $F_{\mu\nu\lambda}$, forming a metric-skew-tensor-gravity (MSTG) theory. We shall apply this gravity theory to explain the flat rotation curves of galaxies and cluster lensing without postulating exotic dark matter. Since no dark matter has been detected so far, it seems imperative to seek a possible modified gravitational theory that could explain the now large amount of data on galaxy rotation curves. A cosmological model obtained from the field equations and a running of the effective gravitational coupling constant G in the matter epoch could explain the growth of large scale structure formation without invoking cold dark matter. The running of the cosmological constant would produce a quintessence-like dark energy that could account for the acceleration of the expansion of the universe [5, 6, 7].

A renormalization group (RG) framework [8] for MSTG is developed to describe the running of the effective gravitational coupling constant G , and the effective coupling constant γ_c that measures the strength of the coupling of the $F_{\mu\nu\lambda}$ field to matter. A momentum cutoff identification $k = k(x)$ associates the RG scales to points in spacetime. For the weak field static, spherically symmetric solution the RG flow equations allow a running with momentum k and distance $\ell = 1/k$ for the effective Newtonian coupling constant $G = G(r)$, the coupling constant $\gamma_c = \gamma_c(r)$, and the effective mass of the skew field $\mu = \mu(r)$ where r denotes the radial coordinate. The form of $G(r)$ as a function of r , obtained from the modified Newtonian acceleration law, leads to agreement with solar system observations, terrestrial gravitational experiments and the binary pulsar PSR 1913+16 observations, while strong renormalization effects in the infrared regime at large distances lead to fits to galaxy rotation curves.

A fit to both low surface brightness and high surface brightness galaxies is achieved in terms of the total galaxy mass M (or M/L) without exotic dark matter. A satisfactory fit is achieved to the rotational velocity data generic to the elliptical galaxy NGC 3379. Fits to the data of the two spheroidal dwarf galaxies Fornax and Draco and the globular cluster ω Centauri are also obtained. The predicted light bending and lensing can lead to agreement with galaxy cluster lensing observations. A model of the modified acceleration law that includes a description of radial velocity curves in the core of galaxies as well as in the outer regions of the galaxy is shown to yield good fits to rotational velocity data.

For a homogeneous and isotropic universe, based on the Friedmann- Lemaitre- Robertson-Walker (FLRW) model, the average value of the skew symmetric field $F_{\mu\nu\lambda}$ is zero. However, for an effective gravitational constant $G = G(t)$ that runs with time, we find that the constraint $G(t) \sim G_0$ (where G_0 is Newton's constant, $G_0 = 6.673 \times 10^{-8} \text{ g}^{-1} \text{ cm}^3 \text{ sec}^{-2}$) must be imposed on $G(t)$ at the time of big bang nucleosynthesis (BBN) and the surface of last scattering (decoupling) when the fraction of baryons is $\Omega_B \sim 0.04$. For a rapid increase of $G(t)$ after the time of decoupling when $G(t)$ reaches a value $G(t) \sim 6G_0$, the matter fraction becomes $\Omega_M \sim 6\Omega_B \sim 0.24$ and there is no need for undetected cold dark matter.

2 The Field Equations

The action for the MSTG theory is given by

$$S = S_G + S_F + S_{FM} + S_M, \quad (1)$$

where S_G is the Einstein-Hilbert action (we choose units such that $c = 1$):

$$S_G = \frac{1}{16\pi G} \int d^4x \sqrt{-g} (R - 2\Lambda), \quad (2)$$

where $g = \text{Det}(g_{\mu\nu})$, $g_{\mu\nu}$ is the symmetric metric tensor of pseudo-Riemannian geometry, $R = g^{\mu\nu} R_{\mu\nu}$ is the Ricci scalar and Λ is the cosmological constant. Moreover, S_F is the skew field action

$$S_F = \int d^4x \sqrt{-g} \left(\frac{1}{12} F_{\mu\nu\rho} F^{\mu\nu\rho} - \frac{1}{4} \mu^2 A_{\mu\nu} A^{\mu\nu} \right), \quad (3)$$

where

$$F_{\mu\nu\lambda} = \partial_\mu A_{\nu\lambda} + \partial_\nu A_{\lambda\mu} + \partial_\lambda A_{\mu\nu}, \quad (4)$$

and μ is the mass of the skew field. The gravitational constant G in the action S_G is defined in terms of the “bare” gravitational constant G_0 :

$$G = G_0 Z, \quad (5)$$

where Z corresponds to a “renormalization” of G .

The actions S_M and S_F satisfy the relations

$$\frac{1}{\sqrt{-g}} \frac{\delta S_M}{\delta g^{\mu\nu}} = -\frac{1}{2} T_{M\mu\nu}, \quad \frac{1}{\sqrt{-g}} \frac{\delta S_F}{\delta g^{\mu\nu}} = -\frac{1}{2} T_{F\mu\nu}. \quad (6)$$

Moreover, we have

$$\frac{\delta S_{FM}}{\delta A^{\mu\nu}} = -J_{\mu\nu}. \quad (7)$$

Here, $T_{M\mu\nu}$ is the energy-momentum tensor for matter, while $T_{F\mu\nu}$ is the energy-momentum tensor containing the contributions from the massive skew field $A_{\mu\nu}$. Also, $J_{\mu\nu}$ is the tensor density source for the $A_{\mu\nu}$ field.

A possible action for the skew field matter coupling is [9]:

$$S_{FM} = \int d^4x F_{\lambda\mu\nu} J^{*\lambda\mu\nu} = -3 \int d^4x \epsilon^{\alpha\beta\mu\nu} A_{\alpha\beta} \partial_\mu J_\nu, \quad (8)$$

where J_μ is a vector current that can be conserved and $J^{*\mu\nu\lambda} = \epsilon^{\mu\nu\lambda\alpha} J_\alpha$ is the dual tensor current density. The Levi-Civita symbol $\epsilon^{\mu\nu\lambda\alpha}$ transforms as a contravariant tensor density, while $\epsilon^{\mu\nu\lambda\alpha} = \pm 1, 0$. The Pauli coupling (8) is gauge invariant for any J_μ . The source current can be identified with a matter fermion current associated with baryon and lepton number.

The field equations derived from the action principle are given by

$$G_{\mu\nu} + \Lambda g_{\mu\nu} = 8\pi G T_{\mu\nu}, \quad (9)$$

$$\nabla^\sigma F_{\mu\nu\sigma} + \mu^2 A_{\mu\nu} = \frac{1}{\sqrt{-g}} J_{\mu\nu}, \quad (10)$$

where $G_{\mu\nu} = R_{\mu\nu} - \frac{1}{2}g_{\mu\nu}R$, $T_{\mu\nu} = T_{M\mu\nu} + T_{F\mu\nu}$ and ∇^σ denotes the covariant derivative with respect to $g_{\mu\nu}$. Moreover, we have

$$J_{\mu\nu} = \epsilon_{\mu\nu\alpha\beta} \partial^\alpha J^\beta. \quad (11)$$

The Bianchi identities satisfied by the Einstein tensor $G^{\mu\nu}$ lead to the conservation laws

$$\nabla_\nu T^{\mu\nu} = 0. \quad (12)$$

3 Equations of Motion of Test Particles

The equations of motion for a test particle are given by

$$\frac{du^\mu}{d\tau} + \left\{ \begin{array}{c} \mu \\ \alpha\beta \end{array} \right\} u^\alpha u^\beta = g^{\mu\alpha} f_{\alpha\nu} u^\nu, \quad (13)$$

where τ is the proper time along the path of the particle and $u^\lambda = dx^\lambda/d\tau$ is the 4-velocity of the particle. Moreover,

$$\left\{ \begin{array}{c} \lambda \\ \mu\nu \end{array} \right\} = \frac{1}{2} g^{\lambda\rho} (g_{\mu\rho,\nu} + g_{\rho\nu,\mu} - g_{\mu\nu,\rho}), \quad (14)$$

is the Christoffel connection and

$$f_{\alpha\mu} = \lambda \partial_{[\alpha} \left(\frac{\epsilon^{\eta\sigma\nu\lambda}}{\sqrt{-g}} H_{\sigma\nu\lambda} g_{\mu]\eta} \right). \quad (15)$$

Here, $H_{\mu\nu\lambda}$ is given by

$$H_{\mu\nu\lambda} = \frac{1}{3} (\partial_\lambda A_{\mu\nu} + \partial_\mu A_{\nu\lambda} + \partial_\nu A_{\lambda\mu}), \quad (16)$$

and λ is a coupling constant with the dimension of length that couples the skew field to the test particle.

For a spherically symmetric, static skew symmetric potential field $A_{\mu\nu}$ there are two non-vanishing components, the “magnetic” field potential $A_{0r}(r) = w(r)$ and the “electric” potential field $A_{\theta\phi}(r) = f(r) \sin \theta$. We shall assume that only the electric field contribution $f(r) \sin \theta$ is non-zero (no static magnetic poles). Then, the tensor $H_{\mu\nu\lambda}$ has only one non-vanishing component:

$$H_{\theta\phi r} = \frac{1}{3} \partial_r A_{\theta\phi} = f' \sin \theta, \quad (17)$$

where $f' = df/dr$. We obtain

$$f_{r0} = \lambda \frac{d}{dr} \left(\frac{\gamma f'}{\sqrt{\alpha \gamma r^4}} \right). \quad (18)$$

For a static spherically symmetric gravitational field the line element is

$$ds^2 = \gamma(r)dt^2 - \alpha(r)dr^2 - r^2(d\theta^2 + \sin^2 \theta d\phi^2). \quad (19)$$

The equations of motion for a test particle are given by

$$\begin{aligned} \frac{d^2r}{d\tau^2} + \frac{\alpha'}{2\alpha} \left(\frac{dr}{d\tau} \right)^2 - \frac{r}{\alpha} \left(\frac{d\theta}{d\tau} \right)^2 - r \left(\frac{\sin^2 \theta}{\alpha} \right) \left(\frac{d\phi}{d\tau} \right)^2 + \frac{\gamma'}{2\alpha} \left(\frac{dt}{d\tau} \right)^2 \\ + \frac{1}{\alpha} \frac{d}{dr} \left(\frac{\lambda \gamma f'}{\sqrt{\alpha \gamma r^4}} \right) \left(\frac{dt}{d\tau} \right) = 0, \end{aligned} \quad (20)$$

$$\frac{d^2t}{d\tau^2} + \frac{\gamma'}{\gamma} \left(\frac{dt}{d\tau} \right) \left(\frac{dr}{d\tau} \right) + \frac{1}{\gamma} \frac{d}{dr} \left(\frac{\lambda \gamma f'}{\sqrt{\alpha \gamma r^4}} \right) \left(\frac{dr}{d\tau} \right) = 0, \quad (21)$$

$$\frac{d^2\theta}{d\tau^2} + \frac{2}{r} \left(\frac{d\theta}{d\tau} \right) \left(\frac{dr}{d\tau} \right) - \sin \theta \cos \theta \left(\frac{d\phi}{d\tau} \right)^2 = 0, \quad (22)$$

$$\frac{d^2\phi}{d\tau^2} + \frac{2}{r} \left(\frac{d\phi}{d\tau} \right) \left(\frac{dr}{d\tau} \right) + 2 \cot \theta \left(\frac{d\phi}{d\tau} \right) \left(\frac{d\theta}{d\tau} \right) = 0. \quad (23)$$

The orbit of the test particle can be shown to lie in a plane and by an appropriate choice of axes, we can make $\theta = \pi/2$. Integrating Eq.(23) gives

$$r^2 \frac{d\phi}{d\tau} = J, \quad (24)$$

where J is the conserved orbital angular momentum. Integration of Eq.(21) gives

$$\frac{dt}{d\tau} = -\frac{1}{\gamma} \left[\frac{\lambda \gamma f'}{\sqrt{\alpha \gamma r^4}} + E \right], \quad (25)$$

where E is the constant energy per unit mass.

By substituting (25) into (20) and using (24), we obtain

$$\frac{d^2r}{d\tau^2} + \frac{\alpha'}{2\alpha} \left(\frac{dr}{d\tau} \right)^2 - \frac{J^2}{\alpha r^3} + \frac{\gamma'}{2\alpha \gamma^2} \left(\frac{\lambda \gamma f'}{\sqrt{\alpha \gamma r^4}} + E \right)^2 = \frac{1}{\alpha \gamma} \frac{d}{dr} \left(\frac{\lambda \gamma f'}{\sqrt{\alpha \gamma r^4}} \right) \left(\frac{\lambda \gamma f'}{\sqrt{\alpha \gamma r^4}} + E \right). \quad (26)$$

We do not have an exact spherically symmetric, static solution for massive MSTG. For large enough values of r , we shall approximate the metric components α and γ by the Schwarzschild solution:

$$\alpha(r) \sim \frac{1}{1 - \frac{2GM}{r}}, \quad \gamma(r) \sim 1 - \frac{2GM}{r}, \quad (27)$$

and make the approximations that $2GM/r \ll 1$, $\lambda f'/r^2 \ll 1$, $f/r^2 \ll 1$ and the slow motion approximation $dr/dt \ll 1$. Then, for material particles we set $E = 1$ and (26) becomes

$$\frac{d^2r}{dt^2} - \frac{J_N^2}{r^3} + \frac{GM}{r^2} = \lambda \frac{d}{dr} \left(\frac{f'}{r^2} \right), \quad (28)$$

where J_N is the Newtonian orbital angular momentum.

4 Linear Weak Field Approximation

We expand $g_{\mu\nu}$ about a Minkowski flat spacetime

$$g_{\mu\nu} = \eta_{\mu\nu} + h_{\mu\nu} + O(h^2), \quad (29)$$

where $\eta_{\mu\nu} = \text{diag}(1, -1, -1, -1)$ is the Minkowski metric tensor. The skew field $F_{\mu\nu\lambda}$ obeys the linearized equations of motion for empty space

$$\partial^\sigma F_{\mu\nu\sigma} + \mu^2 A_{\mu\nu} = 0. \quad (30)$$

These are the massive Kalb-Ramond-Proca equations [10], which are free of ghost pole instabilities and possess a positive Hamiltonian bounded from below.

The equations (30) for a static spherically symmetric field become

$$f''(r) - \frac{2}{r} f'(r) - \mu^2 f(r) = 0, \quad (31)$$

and have the solution

$$f(r) = \frac{1}{3} s G^2 M^2 \exp(-\mu r) (1 + \mu r), \quad (32)$$

where s is a dimensionless constant.

To the order of weak field approximation, we obtain from Eqs.(28) and (32):

$$\frac{d^2 r}{dt^2} - \frac{J_N^2}{r^3} = -\frac{GM}{r^2} + \frac{\sigma \exp(-\mu r)}{r^2} (1 + \mu r), \quad (33)$$

where the constant σ is given by

$$\sigma = \frac{\lambda s G^2 M^2 \mu^2}{3}. \quad (34)$$

We have required in Eq.(33) that the additional acceleration on the right-hand side is a repulsive force. This is in keeping with the identification of $A_{\mu\nu}$ with the potential field of a massive axial vector 1^+ boson.

An analysis of the physical properties of a massive spin 1^+ boson exchange was carried out by Damour, Deser and McCarthy (DDM) [9], based on a modification of a massive NGT with skew field $B_{\mu\nu}$. In a version of a rigorous massive NGT [3, 4], the weak field solution for a massive Kalb-Ramond field [10] follows consistently from a weak field approximation to the rigorous NGT field equations and leads to a stable vacuum without ghost energy modes.

The macroscopic coupling action for the DDM skew symmetric $B_{\mu\nu}$ field is given in their notation by

$$S_J = -\frac{1}{6} f_c \int d^4 x H_{\lambda\mu\nu} J^{*\lambda\mu\nu} = \frac{1}{2} f_c \int d^4 x \epsilon^{\mu\nu\alpha\beta} B_{\alpha\beta} \partial_\mu J_\nu, \quad (35)$$

where f_c denotes a dimensionless coupling constant, $H_{\lambda\mu\nu}$ is the fully skew symmetric field strength and J^μ is a current vector that can be conserved. Moreover, $J^{*\lambda\mu\nu} = \epsilon^{\lambda\mu\nu\alpha} J_\alpha$ is a totally antisymmetric tensor density. The action S_J (within trivial numerical factors) is the same action (8) that we have used to obtain our field equations (10) for the $A_{\mu\nu}$ potential field and the equations of motion of a test particle (13). DDM show that the lowest order matter coupling of the skew B-field corresponds to a vector particle “fifth force” coupled to the current J^μ , which can be identified with a fermion current with the dimensionless coupling $g_5 = \sqrt{4\pi G_0} \mu f_c$. Note that the coupling constant g_5 is inversely proportional to the range of the fifth force.

We can consider the strength of the skew field coupling by introducing the coupling constant

$$\lambda_c \equiv \frac{f_c}{m_N} \sim 2f_c \times 10^{-14} \text{ cm}, \quad (36)$$

where m_N is the nucleon mass (one atomic mass unit). Moreover, λ_c has dimensions of a length and couples baryon number to $m_N J^\mu$.

The coupling constant λ_c can be expressed in terms of $\alpha_5 = g_5^2/(4\pi m_N^2)$ as

$$\lambda_c = \frac{\sqrt{\alpha_5}}{\mu} = \sqrt{\alpha_5} r_0, \quad (37)$$

where $r_0 = 1/\mu$ is the range of the force. This show that λ_c can take large macroscopic values provided that the range r_0 is large enough. In our RG flow framework, the coupling constant λ_c will run and become increasingly large in the IR momentum limit $k \rightarrow 0$, corresponding to increasing values of the range r_0 . We can define a “renormalized” coupling constant

$$\lambda_c = \lambda_{c0} A, \quad (38)$$

where λ_{c0} is the bare skew field coupling constant and A is a renormalization constant.

Experiments have put stringent bounds on possible fifth forces and the magnitude of g_5 [11]. However, DDM make the important points for phenomenological purposes that the strength of the coupling f_c is unbounded as the range increases, and that the magnitude of the B-field (in our notation the B-field is $A_{\mu\nu}$) is primarily proportional to f_c and independent of the range r_0 . This allows the B-field to have a “gravitational” strength, while still keeping compatibility with the existing stringent bounds on possible violations of the weak equivalence principle and composition-dependent effects in Newtonian gravity.

It should be noted that significant observational bounds on fifth forces only apply to distances $\leq 1 \text{ a.u.}$ in the solar system, corresponding to $\mu \leq 10^{-18} \text{ eV}$. The experiments do not place useful bounds on the strength of the coupling of a gravitational fifth force at galactic distance scales $\sim 5 - 100 \text{ kpc}$ or at cosmological scales. This is in keeping with the requirement that our modified acceleration law

will be approximately Newtonian at distance scales within the solar system, and that the NGT predictions for solar system distance scales agree with the solar system observations.

5 Orbital Equation of Motion

We set $\theta = \pi/2$ in (19), divide the resulting expression by $d\tau^2$ and use Eqs.(24) and (25) to obtain

$$\left(\frac{dr}{d\tau}\right)^2 + \frac{J^2}{\alpha r^2} - \frac{1}{\alpha\gamma} \left[\frac{\lambda\gamma f'}{\sqrt{\alpha\gamma r^4}} + E \right]^2 = -\frac{E}{\alpha}. \quad (39)$$

We have $ds^2 = Ed\tau^2$, so that $ds/d\tau$ is a constant. For material particles $E > 0$ and for massless photons $E = 0$.

Let us set $u = 1/r$ and by using (24), we have $dr/d\tau = -Jdu/d\phi$. Substituting this into (39), we obtain

$$\left(\frac{du}{d\phi}\right)^2 = \frac{1}{\alpha\gamma J^2} \left[E + \frac{\lambda\gamma f'}{\sqrt{\alpha\gamma r^4}} \right]^2 - \frac{1}{\alpha r^2} - \frac{E}{\alpha J^2}. \quad (40)$$

By substituting (27) and $dr/d\phi = -(1/u^2)du/d\phi$ into (40), we get after some manipulation:

$$\frac{d^2u}{d\phi^2} + u = \frac{EGM}{J^2} - \frac{E\lambda s G^2 M^2}{3r_0^2 J^2} \exp\left(-\frac{1}{r_0 u}\right) \left(1 + \frac{1}{r_0 u}\right) + 3GMu^2, \quad (41)$$

where $r_0 = 1/\mu$.

For material test particles $E = 1$ and we obtain

$$\frac{d^2u}{d\phi^2} + u = \frac{GM}{J^2} + 3GMu^2 - \frac{K}{J^2} \exp\left(-\frac{1}{r_0 u}\right) \left(1 + \frac{1}{r_0 u}\right), \quad (42)$$

where $K = \lambda s G^2 M^2 / 3r_0^2$. On the other hand, for massless photons $ds^2 = 0$ and $E = 0$ and (41) gives

$$\frac{d^2u}{d\phi^2} + u = 3GMu^2. \quad (43)$$

6 Galaxy Rotational Velocity Curves

A possible explanation of the galactic rotational velocity curves problem has been obtained in NGT [12]. We shall now obtain an equivalent explanation of the rotational velocity curves from the present MSTG theory. From the radial acceleration derived from (33) experienced by a test particle in a static, spherically symmetric gravitational field due to a point source, we obtain

$$a(r) = -\frac{G_\infty M}{r^2} + \sigma \frac{\exp(-r/r_0)}{r^2} \left(1 + \frac{r}{r_0}\right). \quad (44)$$

Here, G_∞ is defined to be the *effective* gravitational constant at infinity

$$G_\infty = G_0 \left(1 + \sqrt{\frac{M_0}{M}} \right), \quad (45)$$

where G_0 is Newton's "bare" gravitational constant. This conforms with our definition of G in Eq.(5), which requires that the effective G be renormalized in order to guarantee that (44) reduces to the Newtonian acceleration

$$a_{\text{Newton}} = -\frac{G_0 M}{r^2} \quad (46)$$

at small distances $r \ll r_0$. The constant σ is given by

$$\sigma = \frac{\lambda s G_0^2 M^2}{3c^2 r_0^2}. \quad (47)$$

The integration constant s in (47) is dimensionless and can be modelled as

$$s = gM^a, \quad (48)$$

where M is the total mass of the particle source, g is a coupling constant and a is a dimensionless constant. We choose $a = -3/2$ and set $\lambda g G_0 / 3c^2 r_0^2 = \sqrt{M_0}$ where M_0 is a parameter. The choice of $a = -3/2$ yields for galaxy dynamics an approximate Tully-Fisher law [15].

We obtain the acceleration on a point particle

$$a(r) = -\frac{G_\infty M}{r^2} + G_0 \sqrt{M M_0} \frac{\exp(-r/r_0)}{r^2} \left(1 + \frac{r}{r_0} \right). \quad (49)$$

By using (45), we can express the modified acceleration in the form

$$a(r) = -\frac{G_0 M}{r^2} \left\{ 1 + \sqrt{\frac{M_0}{M}} \left[1 - \exp(-r/r_0) \left(1 + \frac{r}{r_0} \right) \right] \right\}. \quad (50)$$

In section 10, we shall explain the running with distance scale of the effective gravitational constant $G = G(r)$ and the skew field coupling constant $s = s(r)$ in an RG flow, effective MSTG action framework in which RG phase space trajectories possess Gaussian and non-Gaussian fixed points. We can rewrite (50) in the form

$$a(r) = -\frac{G(r) M}{r^2}, \quad (51)$$

where

$$G(r) = G_0 \left\{ 1 + \sqrt{\frac{M_0}{M}} \left[1 - \exp(-r/r_0) \left(1 + \frac{r}{r_0} \right) \right] \right\}. \quad (52)$$

Thus, $G(r)$ describes the running with distance of the effective gravitational constant in the RG flow scenario.

We apply (50) to explain the flatness of rotation curves of galaxies, as well as the approximate Tully-Fisher law [15], $v^4 \propto G_0 M \propto L$, where v is the rotational velocity of a galaxy, M is the galaxy mass

$$M = M_* + M_{HI} + M_{DB} + M_f, \quad (53)$$

and L is the galaxy luminosity. Here, M_* , M_{HI} , M_{DB} and M_f denote the visible mass, the mass of neutral hydrogen, possible dark baryon mass and gas, and the mass from the skew field energy density, respectively. The mass M_f obtained from the skew field density ρ_f is expected to contribute a small amount to the total mass M of galaxies.

The rotational velocity of a star v obtained from $v^2(r)/r = a(r)$ is given by

$$v = \sqrt{\frac{G_0 M}{r}} \left\{ 1 + \sqrt{\frac{M_0}{M}} \left[1 - \exp(-r/r_0) \left(1 + \frac{r}{r_0} \right) \right] \right\}^{1/2}. \quad (54)$$

Let us postulate that the parameters M_0 and r_0 give the magnitude of the constant acceleration

$$a_0 = \frac{G_0 M_0}{r_0^2}. \quad (55)$$

We assume that for galaxies and clusters of galaxies this acceleration is determined by

$$a_0 = c H_0. \quad (56)$$

Here, H_0 is the current measured Hubble constant $H_0 = 100 h \text{ km s}^{-1} \text{ Mpc}^{-1}$ where $h = (0.71 \pm 0.07)$ [13]. This gives

$$a_0 = 6.90 \times 10^{-8} \text{ cm s}^{-2}. \quad (57)$$

We note that $a_0 = c H_0 \sim (\sqrt{\Lambda/3})c^2$, so there is an interesting connection between the parameters M_0 , r_0 and the cosmological constant Λ .

A good fit to low surface brightness and high surface brightness galaxy data is obtained with the parameters

$$M_0 = 9.60 \times 10^{11} M_\odot, \quad r_0 = 13.92 \text{ kpc} = 4.30 \times 10^{22} \text{ cm} \quad (58)$$

and M (or the mass-to-light ratio M/L). By using (57) and substituting $M_0 = 9.60 \times 10^{11} M_\odot$ into (55), we obtain the r_0 in (58). Thus, we fit the galaxy rotation curve data with one parameter M_0 and the total galaxy mass M . Since we are using an equation of motion for point particle sources, we are unable to fit the cores of galaxies without supplementing the acceleration formula with a galaxy core model based on a mass distribution.

Let us now describe a model of a spherically symmetric galaxy with a core density of visible matter, $\rho_c(r)$, within a core radius $r < r_c$. The acceleration law takes the form

$$a(r) = -\frac{G_0 M(r)}{r^2} \left\{ 1 + \sqrt{\frac{M_0}{M}} \left[1 - \exp(-r/r_0) \left(1 + \frac{r}{r_0} \right) \right] \right\}, \quad (59)$$

where

$$\mathcal{M}(r) = 4\pi \int_0^r dr' r'^2 \rho_c(r') \quad (60)$$

is the ordinary matter inside the luminous core of the galaxy described by a ball of radius $r = r_c$. Inside the core radius r_c the dynamics is described by Newtonian theory. Moreover, the acceleration outside the core radius $r > r_c$ is described by (50), while M is determined by (53). A simple model for $\mathcal{M}(r)$ is given by¹

$$\mathcal{M}(r) = M \left(\frac{r}{r_c + r} \right)^2. \quad (61)$$

The rotational velocity derived from the acceleration law (59) is

$$v = \sqrt{\frac{G_0 M}{r}} \left(\frac{r}{r_c + r} \right) \left\{ 1 + \sqrt{\frac{M_0}{M}} \left[1 - \exp(-r/r_0) \left(1 + \frac{r}{r_0} \right) \right] \right\}^{1/2}. \quad (62)$$

The modified acceleration law (59) can be compared to the Newtonian law using (61):

$$a_{\text{Newton}}(r) = -\frac{G_0 \mathcal{M}(r)}{r^2}. \quad (63)$$

The fits to the galaxy rotation curves v in km/s versus the galaxy radius r in kpc are shown in Fig. 1. The acceleration law is given for point particles by (50). The data are obtained from ref. [14].

In Fig. 2, fits to two dwarf galaxies (dSph) are shown. We assume that the relation between the velocity dispersion σ and the rotational velocity v takes the simple form in e.g. an isothermal sphere model for which $v \sim \sqrt{2}\sigma$. The error bars on the data [16] for the velocity dispersions are large, and in the case of Draco, due to the small radial range $0.1 \text{ kpc} < r < 0.6 \text{ kpc}$, the Newtonian curve for

$$v = \sqrt{\frac{G_0 M}{r}}, \quad (64)$$

cannot be distinguished within the errors from the NGT prediction. However, it is noted that the NGT prediction for v appears to flatten out as r increases. For Draco $M/L = 28.93 + 50.30(9.58)(M_\odot/L_\odot)$, whereas for Fornax $M/L = 1.79 + 0.72(0.40)(M_\odot/L_\odot)$. There is also an expected large error in the distance estimates to the dSph. Another serious potential source of error is that it is assumed that dSph galaxies are in dynamical equilibrium. The two studied here are members of the Local Group and exist in the gravitational field of a larger galaxy, the Milky Way. Thus, the tidal interactions with the larger galaxy are expected to affect the dynamics of dSph galaxies and the interpretations of velocity dispersions [17]. These

¹We can choose to solve a Poisson equation for the potential that gives a more accurate description of the core behavior of the galaxy, including bulge effects and other detailed features of the galaxy associated with a measured luminosity distribution. However, the model considered here yields a reasonable description of the velocity curves in the core regions of the galaxies.

issues and others for dSph galaxies are critically considered in the context of dark matter models by Kormendy and Freeman [18].

We have also included a fit to the elliptical galaxy NGC 3379. The elliptical galaxy NGC 3379 has been the source of controversy recently [19]. The velocities of elliptical galaxies are randomly distributed in the galaxy. However, the gravitational potential that would be experienced by a test particle star or planetary nebula in circular rotation about the center of the galaxy can be extracted from the line-of-sight velocity dispersion profiles. The data for $R/R_{\text{eff}} > 0.5$ refer to planetary nebula.

We use the mean values of the extracted rotational velocities for NGC 3379, obtained by Romanowsky et al. [19] and find that our predicted rotational velocities agree well with their data. According to Romanowsky et al. there appears to be a dearth of dark matter in the elliptical galaxy which needs to be explained by dark matter models and N-body cosmological simulations. For Milgrom's MOND [20, 21] it is argued by Sanders and Milgrom [22] that NGC 3379 is marginally outside the MOND regime with an acceleration $a \sim (a_0)_{\text{Milgrom}} \sim 1.2 \times 10^{-8} \text{ cm s}^{-2}$, so the MOND prediction for elliptical galaxies should be closer to the Newtonian-Kepler prediction for the rotational velocity curve. Romanowsky et al. also give data for the two elliptical galaxies NGC 821 and NGC 4494, but the intrinsic circular velocities inferred from the line-of-sight velocity dispersion profile data are not given by the authors, although the trends of the data are similar to NGC 3379.

A fit to the data for the globular cluster ω Centauri is shown in Fig. 3. The data is from McLaughlin and Meylan [23]. We use the velocity dispersion data and assume that the data is close to the rotational velocity curves associated with the velocity dispersion σ_p i.e. the isothermal sphere model relation $v \sim \sqrt{2}\sigma_p$ holds. The fit to the data reveals that the predicted rotational velocity cannot be distinguished from the Newtonian-Kepler circular velocity curve within the orbital radius of the data. The authors conclude that there appears to be no room for dark matter, whereas the our results agree well with the data. For Milgrom's MOND, the magnitude of the acceleration is larger than the MOND upper limit $(a_0) \sim 10^{-8} \text{ cm /sec}$ and we expect to obtain a Newtonian-Kepler rotation curve.

In Fig. 4, we show fits to the four galaxies NGC 1560, NGC 2903, NGC 4565 and NGC 5055 using the modified acceleration law (59) including the galaxy core. As can be seen from the data fitting, the agreement with the core and extended rotation curves data [24, 25] is good for the two fitting parameters M and the core radius r_c .

In Fig. 5, we display a 3-dimensional plot of v versus the range of distance $0.1 \text{ kpc} < r < 10 \text{ kpc}$ and the range of total galaxy mass M used in the fitting of rotational velocity data. The red surface shows the Newtonian values of the rotational velocity v , while the black surface displays the prediction for v obtained from our gravity theory.

Table 1 displays the values of the total mass M used to fit the galaxies and the mass-to-light ratios M/L estimated from the data in references given in [14], using

the non-core acceleration model (50).

In Milgrom's phenomenological model [20, 21] we have

$$v^4 = G_0 M (a_0)_{\text{Milgrom}}, \quad (65)$$

where $(a_0)_{\text{Milgrom}} = 1.2 \times 10^{-8} \text{ cm s}^{-2}$. We see that (65) predicts that the rotational velocity is constant out to an infinite range and the rotational velocity does not depend on a distance scale, but on the magnitude of the acceleration $(a_0)_{\text{Milgrom}}$ ². In contrast, our modified acceleration formula does depend on the radius r and the distance scale r_0 which for galaxies is fixed by the formula (56). The MSTG velocity curve asymptotically becomes the same as the Newtonian-Kepler prediction as $r \rightarrow \infty$:

$$v \sim \sqrt{G_\infty M/r}, \quad (66)$$

where G_∞ is the renormalized value of Newton's constant.

Using the Sloan Digital Sky Survey (SDSS), Prada et al. [26] have studied the velocities of satellites orbiting isolated galaxies. They detected approximately 3000 satellites, and they found that the line-of-sight velocity dispersion of satellites declines with distance to the primary. The velocity was observed to decline to a distance of ~ 350 kpc for the available data. This result contradicts the constant velocity prediction (65) of MOND, but agrees with the MSTG prediction (66). It also agrees with the cosmological models which predict mass profiles of dark matter halos at large distances. During the last two decades of numerical modelling of galaxy formation, they have produced a density profile of dark matter halos, $\rho \propto 1/r^3$ at large radii, which does not depend on the nature of the dark matter [27].

7 Local and Solar System Observations

We obtain from Eq.(42) the orbit equation

$$\frac{d^2u}{d\phi^2} + u = \frac{GM}{c^2 J^2} - \frac{K}{J^2} \exp(-r/r_0) \left[1 + \left(\frac{r}{r_0} \right) \right] + \frac{3GM}{c^2} u^2, \quad (67)$$

where now $K = \lambda s G^2 M^2 / 3c^4 r_0^2$. Using the large r weak field approximation, and the expansion

$$\exp(-r/r_0) = 1 - \frac{r}{r_0} + \frac{1}{2} \left(\frac{r}{r_0} \right)^2 + \dots \quad (68)$$

we obtain the orbit equation for $r \ll r_0$:

$$\frac{d^2u}{d\phi^2} + u = N + 3 \frac{GM}{c^2} u^2, \quad (69)$$

²In formulations of Milgrom's model, the modified Newtonian potential has a logarithmic dependence on r

where

$$N = \frac{GM}{c^2 J_N^2} - \frac{K}{J_N^2}. \quad (70)$$

We can solve Eq.(69) by perturbation theory and find for the perihelion advance of a planetary orbit

$$\Delta\omega = \frac{6\pi}{c^2 L} (GM_\odot - c^2 K_\odot), \quad (71)$$

where $J_N = (GM_\odot L/c^2)^{1/2}$, $L = a(1 - e^2)$ and a and e denote the semimajor axis and the eccentricity of the planetary orbit, respectively.

We now use the running of the effective gravitational coupling constant $G = G(r)$, determined by (52) and find that for the solar system $r \ll r_0 = 14$ kpc, we have $G \sim G_0$ within the experimental errors for the measurement of Newton's constant G_0 . We choose for the solar system $K_\odot \ll 1.5$ km and use $G = G_0$ to obtain from (71) a perihelion advance of Mercury in agreement with GR.

For terrestrial experiments and orbits of satellites, we have also that $G \sim G_0$ for $r \sim r_\oplus$ where $r_\oplus \ll r_0 = 14$ kpc is the radius of Earth. We then achieve agreement with all gravitational terrestrial experiments including Eötvös free-fall experiments and “fifth force” experiments.

For the binary pulsar PSR 1913+16 the formula (71) can be adapted to the periastron shift of a binary system. Combining this with the NGT gravitational wave radiation formula, which will approximate closely the GR formula, we can obtain agreement with the observations for the binary pulsar. The mean orbital radius for the binary pulsar is equal to the projected semi-major axis of the binary, $\langle r \rangle_N = 7 \times 10^{10}$ cm, so that $\langle r \rangle_N \ll 14$ kpc. Thus, $G = G_0$ within the experimental errors and agreement with the binary pulsar data for the periastron shift is obtained for $K_N \ll 4.2$ km.

For a massless photon $E = 0$ and we have

$$\frac{d^2 u}{d\phi^2} + u = 3 \frac{GM}{c^2} u^2. \quad (72)$$

For the solar system using $G = G_0$ within the experimental errors gives the light deflection:

$$\Delta_\odot = \frac{4G_0 M_\odot}{c^2 R_\odot} \quad (73)$$

in agreement with GR.

8 Galaxy Clusters and Lensing

We can assess the existence of dark matter of galaxies and clusters of galaxies in two independent ways: from the dynamical behavior of test particles through the study of extended rotation curves of galaxies, and from the deflection and focusing of electromagnetic radiation, e.g., gravitational lensing of clusters of galaxies. The

light deflection by gravitational fields is a relativistic effect, so the second approach provides a way to test the relativistic effects of gravitation at the extra-galactic level. It has been shown that for conformal tensor-scalar gravity theories the bending of light is either the same or can even be weaker than predicted by GR [21, 28]. To remedy this problem, Bekenstein [21] has recently formulated a relativistic description of Milgrom's MOND model, including a time-like vector field as well as two scalar fields within a GR metric scenario. However, the time-like vector field violates local Lorentz invariance and requires preferred frames of reference.

The bending angle of a light ray as it passes near a massive system along an approximately straight path is given to lowest order in v^2/c^2 by

$$\theta = \frac{2}{c^2} \int |a^\perp| dz, \quad (74)$$

where \perp denotes the perpendicular component to the ray's direction, and dz is the element of length along the ray and a denotes the acceleration. The best evidence in favor of dark matter lensing is the observed luminous arcs seen in the central regions of rich galaxy clusters [29]. The cluster velocity dispersion predicted by the observed arcs is consistent within errors with the observed velocity dispersion of the cluster galaxies. This points to a consistency between the virial mass and the lensing mass, which favors the existence of dark matter.

From (72), we obtain the light deflection

$$\Delta = \frac{4GM}{c^2 R} = \frac{4G_0 \overline{M}}{c^2 R}, \quad (75)$$

where

$$\overline{M} = M \left(1 + \sqrt{\frac{M_0}{M}} \right). \quad (76)$$

The value of \overline{M} follows from (52) for clusters as $r \gg r_0$ and

$$G(r) \rightarrow G_\infty = G_0 \left(1 + \sqrt{\frac{M_0}{M}} \right). \quad (77)$$

We choose for a cluster $M_0 = 9.6 \times 10^{14} M_\odot$ and a cluster mass $M_{\text{cl}} \sim 10^{13} M_\odot$, and obtain

$$\left(\sqrt{\frac{M_0}{M}} \right)_{\text{cl}} \sim 10. \quad (78)$$

We see that $\overline{M} \sim 11M$ and we can explain the increase in the light bending without exotic dark matter.

From the formula Eq.(50) for $r \gg r_0 \sim 14$ kpc we get

$$a(r) = -\frac{G_0 \overline{M}}{r^2}. \quad (79)$$

We expect to obtain from this result a satisfactory description of lensing phenomena using Eq.(74).

The scaling with distance of the renormalized gravitational constant is seen to play an important role in describing consistently the solar system and the galaxy and cluster dynamics, without the postulate of exotic dark matter. In the next section, we outline a framework for an effective, running Newtonian gravitational constant $G = G(k)$ and the skew field coupling constant $\gamma_c(k)$, based on a renormalization group approach to gravity theory.

9 Renormalization Group Flow Gravity Theory and Running Constants

We have postulated a renormalized Newtonian gravitational constant $G = G_0 Z$ in our action Eq.(2), and in the phenomenology for galaxy dynamics

$$Z = 1 + \sqrt{\frac{M_0}{M}}. \quad (80)$$

We shall now implement the running of the effective G and the $F_{\mu\nu\lambda}$ field coupling constant γ_c by using renormalization flow arguments in which the “classical” coupling constants G and γ_c possess a scale dependent running behavior obtained by solving appropriate RG equations. This approach to quantum gravity and its astrophysical implications for the infrared (IR) low energy or large scale dependence of gravity has been applied to Einstein gravity [8, 30, 31, 32] with the intent to explain galaxy rotation curves without dominant dark matter.

We shall postulate scale dependent effective actions $\Gamma_k[g_{\mu\nu}]$ and $\Gamma_k[A_{\mu\nu}]$, corresponding to “coarse-grained” free energy functionals, which define an effective field theory valid at the mass scale k or length scale $\ell = 1/k$. Then the Γ_k are the bare actions obtained by integrating out all quantum fluctuations with momenta larger than an infrared cutoff k_{IR} , or wavelengths smaller than ℓ . The Γ_k are determined by functional differential equations for the RG flow, including the dimensionless coupling constants $\bar{G}(k) = k^2 G(k)$, $\gamma_c(k)$, the cosmological constant $\lambda(k) = \Lambda(k)/k^2$ and the mass $\bar{\mu} = \mu(k)/k$. The dimensionless constant $G(k)\Lambda(k) = \bar{G}(k)\lambda(k)$ is the quantity that is determined by measurement. The flow equations are described by a system of ordinary coupled differential equations:

$$\begin{aligned} k \frac{d}{dk} \bar{G}(k) &= \beta_{\bar{G}}(\bar{G}, \gamma_c, \lambda, \bar{\mu}), & k \frac{d}{dk} \gamma_c(k) &= \beta_{\gamma_c}(\bar{G}, \gamma_c, \lambda, \bar{\mu}), \\ k \frac{d}{dk} \lambda(k) &= \beta_{\lambda}(\bar{G}, \gamma_c, \lambda, \bar{\mu}), & k \frac{d}{dk} \mu(k) &= \beta_{\bar{\mu}}(\bar{G}, \gamma_c, \lambda, \bar{\mu}). \end{aligned} \quad (81)$$

To solve the problem, we are required to restrict the RG flow to a finite-dimensional subspace [8], corresponding to a truncated theory space. In the truncated space

only the coupling constants \bar{G} and γ_c , the cosmological constant λ and the mass $\bar{\mu}$ are considered.

It is assumed that there exists an RG trajectory $(G(k), \gamma_c(k), \Lambda(k), \mu(k))$ and that this gives rise to running coupling constants $G(k), \gamma_c(k)$, a running cosmological constant $\Lambda(k)$ and mass $\mu(k)$ with a cutoff $k = k(x)$. The latter converts the scale dependences of $G(k), \gamma_c(k), \Lambda(k)$ and $\mu(k)$ to a spacetime position dependence [8, 30, 31]:

$$\begin{aligned} G(x) &\equiv G(k = k(x)), \quad \gamma_c(x) \equiv \gamma_c(k = k(x)), \quad \Lambda \equiv \Lambda(k = k(x)), \\ \mu &\equiv \mu(k = k(x)). \end{aligned} \quad (82)$$

We shall follow the procedure of Reuter and Weyer [8, 30, 31] and rewrite the action S_G in (2) as

$$\bar{S}_G = \frac{1}{16\pi G(x)} \int d^4x \sqrt{-g} [R - 2\Lambda(x)], \quad (83)$$

and the skew field action as

$$\bar{S}_F = \int d^4x \sqrt{-g} \left(\frac{1}{12} F_{\mu\nu\rho} F^{\mu\nu\rho} - \frac{1}{4} \mu^2(x) A_{\mu\nu} A^{\mu\nu} \right). \quad (84)$$

We have required the skew field mass $\mu = \mu(x)$ to be a function of the space-time coordinates, allowing for a mass renormalization. The matter action S_M is supplemented by an energy-momentum tensor $\Theta_{\mu\nu}$:

$$\frac{1}{\sqrt{-g}} \left(\frac{\delta S_\Theta}{\delta g^{\mu\nu}} \right) = -\frac{1}{2} \Theta_{\mu\nu}, \quad (85)$$

which describes the energy-momentum associated with the $G(x), \gamma_c(x), \Lambda(x)$ and $\mu(x)$. The new field equations that replace (9) are

$$G_{\mu\nu} + \Lambda g_{\mu\nu} = 8\pi G \bar{T}_{\mu\nu}. \quad (86)$$

The modified energy-momentum tensor $\bar{T}^{\mu\nu}$, which includes the contribution from $\Theta^{\mu\nu}$, must satisfy the generalized Bianchi identities, which follow from the diffeomorphism of the action:

$$\nabla_\nu \bar{T}^{\mu\nu} = 0. \quad (87)$$

These conservation laws lead to constraints on the $\Theta^{\mu\nu}$. The fields $G(x), \gamma_c(x), \Lambda(x)$ and $\mu(x)$ are not varied in the effective actions \bar{S}_G and \bar{S}_F as they are treated as “background external fields” and they do not have corresponding field equations [8, 30, 31]. Thus, the actions do not contain kinetic energy terms corresponding to the fields $G(x), \gamma_c(x), \Lambda(x)$ and $\mu(x)$.

The flow equations are described by the running constants

$$G(k) = \bar{G}(k)/k^2, \quad \gamma_c(k), \quad \Lambda(k) = \lambda k^2, \quad \mu(k) = \bar{\mu}(k)k. \quad (88)$$

Every solution $(\bar{G}(k), \gamma_c(k), \lambda(k), \bar{\mu}(k))$ of the truncated flow equations is associated with the one-parameter family of action functionals

$$\Gamma_k[g_{\mu\nu}] = \frac{1}{16\pi G(k)} \int d^4x \sqrt{-g} [R - 2\Lambda(k)], \quad (89)$$

$$\Gamma_k[A_{\mu\nu}] = \int d^4x \sqrt{-g} \left(\frac{1}{12} F_{\mu\nu\rho} F^{\mu\nu\rho} - \frac{1}{4} \mu^2(k) A_{\mu\nu} A^{\mu\nu} \right). \quad (90)$$

The effective average action formalism follows the RG flow from the bare action $\Gamma_{k=\infty} = S$, corresponding to the initial condition for the Γ_k -flow equation, down to $k = 0$ and $\Gamma_{k=0} = \Gamma$ corresponding to the effective action. We have to solve the effective equations of motion

$$\frac{\delta \Gamma_k[g_{\mu\nu}]}{\delta g_{\mu\nu}} = 0, \quad (91)$$

$$\frac{\delta \Gamma_k[A_{\mu\nu}]}{\delta A_{\mu\nu}} = 0. \quad (92)$$

In practice, we truncate the space of solutions and for the UV sector, simple local truncations are sufficient to describe the physical system, but in the IR limit $k \rightarrow 0$ *nonlocal* terms must be included in the truncation procedure.

We shall presently just consider the running of $G(k)$ and the coupling constant $\gamma_c(k)$. The RG flow equations are dominated by two fixed points \bar{G}_* and $\bar{\gamma}_{c*}$: Gaussian fixed points at $\bar{G}_* = \gamma_{c*} = 0$ and non-Gaussian ones with $\bar{G}_* > 0$ and $\gamma_{c*} > 0$. The high-energy, short distance behavior of the quantum gravity theory is governed by the non-Gaussian fixed points, so that for $k \rightarrow \infty$ all the RG trajectories run into these fixed points and lead to a quantum gravity theory by taking the ultra-violet (UV) cutoff along a trajectory running into the fixed points. This would lead to a non-perturbatively renormalizable quantum gravity theory [33, 34, 35, 36]. The conjectured existence of such a non-perturbatively renormalizable gravity theory still has to be demonstrated.

Both the couplings $G(k)$ and $\gamma_c(k)$ are asymptotically free coupling constants as in quantum chromodynamics (QCD), so that they vanish for $k \rightarrow \infty$. We see that if we interpret $\ell = 1/k$ as a distance scale, then both $G(k)$ and $\gamma_c(k)$ increase all the way from the UV energy scale to the infrared (IR) energy scale as $k \rightarrow 0$. This corresponds to a quantum gravity *anti-screening*, playing the analogous role to the anti-screening in Yang-Mills QCD. The RG trajectory ending at the fixed point $\bar{G}(k=0) = 0$ can be described by the scaling law

$$G(k) = G_0 \left(1 + \frac{g_{IR}}{k^2} \right). \quad (93)$$

This interpolates between the constant Newtonian value $G(k_{\text{lab}}) = G_0$ at large k corresponding to short distances and the increasingly larger values of $G(k)$ at larger distances for small k . The difference between G at $k = 0$ and at a typical laboratory

scale, $k \sim 1/(\text{meter})$ is negligible. Any UV renormalization effects are negligible for laboratory, galaxy and cosmological scales.

The gravitational coupling constant will display a running power law behavior:

$$G(k) = \frac{\bar{G}_*}{k^2}. \quad (94)$$

For the spherically symmetric static solution, the running of $G(r)$ is described by Eq.(52), so that as r increases to galactic distances $G(r)$ increases until it reaches the constant value

$$G_\infty = G_0 \left[1 + \sqrt{\frac{M_0}{M}} \right]. \quad (95)$$

A more detailed analysis of RG flow equations in terms of our effective actions will be presented elsewhere.

We note that if we had considered an effective RG framework based on the Einstein-Hilbert action (2) without including a coupling to the skew field $F_{\mu\nu\lambda\sigma}$, then the weak gravitational field acceleration law would take the effective ‘‘Newtonian form’’ (51). Then, the RG flow effective action formalism is required to predict that $G(r)$ should run in such a way that it produces flat rotation curves for galaxies that fit all the galaxy data [30]. Whether this is possible is a matter of conjecture. In contrast, the running of the effective constant $G = G(r)$ in MSTG theory is determined to a large extent by the field equations of the theory for weak fields and leads to good agreement with the available galaxy rotation curve data.

10 Cosmology Without Cold Dark Matter

We shall assume that the universe is isotropic and homogeneous at large scales and adopt the FLRW line element

$$ds^2 = dt^2 - R^2(t) \left[\frac{dr^2}{1 - kr^2} + r^2(d\theta^2 + \sin^2 \theta d\phi^2) \right]. \quad (96)$$

The Friedmann equations take the form

$$H^2(t) + \frac{k}{R^2(t)} = \frac{8\pi G \rho_M(t)}{3} + \frac{\Lambda}{3}, \quad (97)$$

$$\ddot{R}(t) = -\frac{4\pi G}{3} [\rho_M(t) + 3p_M(t)] R(t) + \frac{\Lambda}{3} R(t), \quad (98)$$

where $H(t) = \dot{R}(t)/R(t)$.

For a homogeneous and isotropic universe the skew symmetric fields $A_{\mu\nu}$ and $F_{\mu\nu\lambda}$ are zero when averaged over large distance scales, since there can be no preferred direction in the maximally symmetric FLRW spacetime. In Eqs. (97) and (98), we have assumed that $G = G_0 Z$ and the renormalized value of G is obtained from

the running of the effective coupling $G = G(t)$ with time. We can write (97) for a spatially flat universe $k = 0$ in the form:

$$\Omega_M(t) + \Omega_\Lambda(t) = 1, \quad (99)$$

where

$$\Omega_M(t) = \frac{8\pi G \rho_M(t)}{3H^2(t)} \quad \Omega_\Lambda = \frac{\Lambda}{3H^2(t)}. \quad (100)$$

We shall impose physical restrictions on the form of the running of $G(t)$. We observe that from calculations of the production of helium and deuterium abundances at the time of BBN [37], it can be shown that $\Omega_B \sim 0.02 - 0.04$. Moreover, from the WMAP data the fractions of baryon and photon densities at the surface of last scattering show that $\Omega_B \sim 0.04$ [7]. Therefore, we must impose the conditions that at the time of nucleosynthesis at $t_{BBN} \sim 10^{-7}$ yrs (at red shift $z \sim 10^9$), $G(t_{BBN}) \sim G_0$ and at the surface of last scattering (decoupling) at $t_{SLS} \sim 10^5$ yrs ($z \sim 10^3$), we require that $G(t_{SLS}) \sim G_0$. Moreover, since the time of the surface of last scattering we additionally require that $G(t)$ grows until the present time to the value $G(t_{\text{now}}) \sim 6G_0$. Given this running of G , it follows that for $t > t_{SLS}$:

$$\Omega_M \sim 6\Omega_B \sim 0.24, \quad (101)$$

and we need only assume a dominant baryon density. Given this scenario, we do not require a dominant cold dark matter in the matter dominated era. There can be small contributions to Ω_M due to massive neutrinos.

A bound on the possible value of a changing G with time is obtained from recent spacecraft measurements [38]:

$$\frac{\dot{G}}{G} = (4 \pm 9) \times 10^{-13} \text{ yr}^{-1}. \quad (102)$$

In order to apply this bound to determine the amount of variation of $G(t)$, we need to know the functional form of $G(t)$ as it runs with time. This must be determined by solving the RG flow equations for our cosmological model. If the running of G with time is such that $\dot{G}/G \sim 0$ for a flat behavior of $G(t) \sim G_0$ up till the surface of last scattering, followed after the surface of last scattering by a rapid rise to $G(t) \sim 6G_0$ with a subsequent value $\dot{G}/G \sim 0$, then the bound (102) will not rule out the required renormalized value $G(t_{\text{now}}) \sim 6G_0$. In Fig. 6, we display a conjectured effective $G(t)$ as a function of t in years that is consistent with (102) and a baryon dominated universe without exotic cold dark matter.

The value of $G(t_{\text{now}}) \sim 6G_0$ required to obtain results consistent with the WMAP data [7] corresponds to cosmological distance scales. For the solar system with a distance scale of order 1-40 a.u., the local value of $G(t_{\text{now}}) \sim G_0$ to within the experimental errors on the measurements of G_0 .

If we take into account the running of the cosmological constant $\Lambda(k)$ in the RG quantum gravity flow framework, then we can have $\Lambda(t)$ run with t in (97) and

(98) and this would correspond to a quintessence scenario [39]. It is possible that the RG flow trajectories that lead to a large distance classical scenario can solve the cosmological constant problem, for these trajectories imply a small cosmological constant [30, 32].

A comparison of our baryon dominated matter era cosmological model with the acoustical peak data obtained from the WMAP observations [7] has to be performed to see whether a satisfactory fit to the data can be obtained. The concordance Λ CDM model agrees well with the data and the present model must produce fits to the CMB data that succeeds as well. Moreover, an investigation of the growth of large scale galaxies and clusters from an initially smooth background of fluctuations must also be performed. Since the effective G in the cosmological model is required to increase after the surface of last scattering to a value $G(t_{\text{now}}) \sim 6G_0$, then we can expect that the gravitational potential well will become deeper and allow for clumping of the baryon matter to form galaxies without cold dark matter. The results of this investigation will be reported elsewhere.

11 Conclusions

We have developed a gravity theory consisting of a metric-skew-tensor action that leads to a modified Newtonian acceleration law that is fitted to galaxy rotation curves. There is a large enough sample of galaxy data which fits our predicted MSTG acceleration law to warrant taking seriously the proposal that the gravity theory can explain the flat rotational velocity curves of galaxies without exotic dark matter. It is interesting to note that we can fit the rotational velocity data of galaxies in the distance range $0.02 \text{ kpc} < r < 70 \text{ kpc}$ and in the mass range $10^5 M_\odot < M < 10^{11} M_\odot$ without exotic dark matter halos [40]. We have also provided a model for the behavior of galaxy rotation curves inside the luminous core of galaxies that predicts well the observed flatness of the rotation curves as the distance from the core increases. The lensing of clusters can also be explained by the theory without exotic dark matter in cluster halos.

Our RG flow effective action description of MSTG quantum gravity allows for a running of the effective G with distance. The RG flow framework for the theory is characterized by special RG trajectories. On the RG trajectory, we identify a regime of distance scales where solar system gravitational physics is well described by GR, which is contained in MSTG as an approximate solution to the field equations. We are able to obtain agreement with the observations in the solar system, terrestrial gravitational experiments and the binary pulsar PSR 1913+16. Strong infrared renormalization effects become visible at the scale of galaxies and the modified Newtonian potential replaces exotic dark matter as an explanation of flat rotation curves. Thus, gravity becomes a “confining force” that has significant predictions for astrophysics and cosmology.

We have demonstrated that the RG flow running of G and MSTG cosmology

can lead to a description of the universe that does not require dominant, exotic dark matter. Dark energy is described by an effective time dependent cosmological constant. A detailed investigation of the MSTG cosmological scenario must be performed to establish that it can describe the large scale structure of the universe, account for galaxy formation and big bang nucleosynthesis and be consistent with the WMAP data. The RG flow trajectories in MSTG in the IR large classical limit can lead to a possible solution to the cosmological constant problem, for they imply a small cosmological constant [8, 32].

The skew fields $F_{\mu\nu\lambda\sigma}$ have a natural interpretation in terms of string theory [10], so that a possible string theory interpretation of the astrophysical predictions can be investigated.

An interesting approach is to solve the MSTG field equations for gravitational collapse to see whether there are any stable massive skew field solutions that correspond to conventional Schwarzschild black holes with event horizons. If the conjectured asymptotically safe renormalizability holds for MSTG quantum gravity, then we might expect that $G(s)$ and $\gamma_c(s)$ vanish as the distance $s = (x \cdot x)^{1/2} \rightarrow 0$, which could lead to a gravitationally-free Minkowski spacetime without singularities at $s = 0$.

Acknowledgments

This work was supported by the Natural Sciences and Engineering Research Council of Canada. I thank Hilary Carteret for help with the use of Maple 9 software and Joel Brownstein, Gilles Esposito-Farése, Laurent Freidel, Arthur Lue, Gary Mamon, Stacey McGough, Martin Green, Martin Reuter and Lee Smolin for helpful discussions.

References

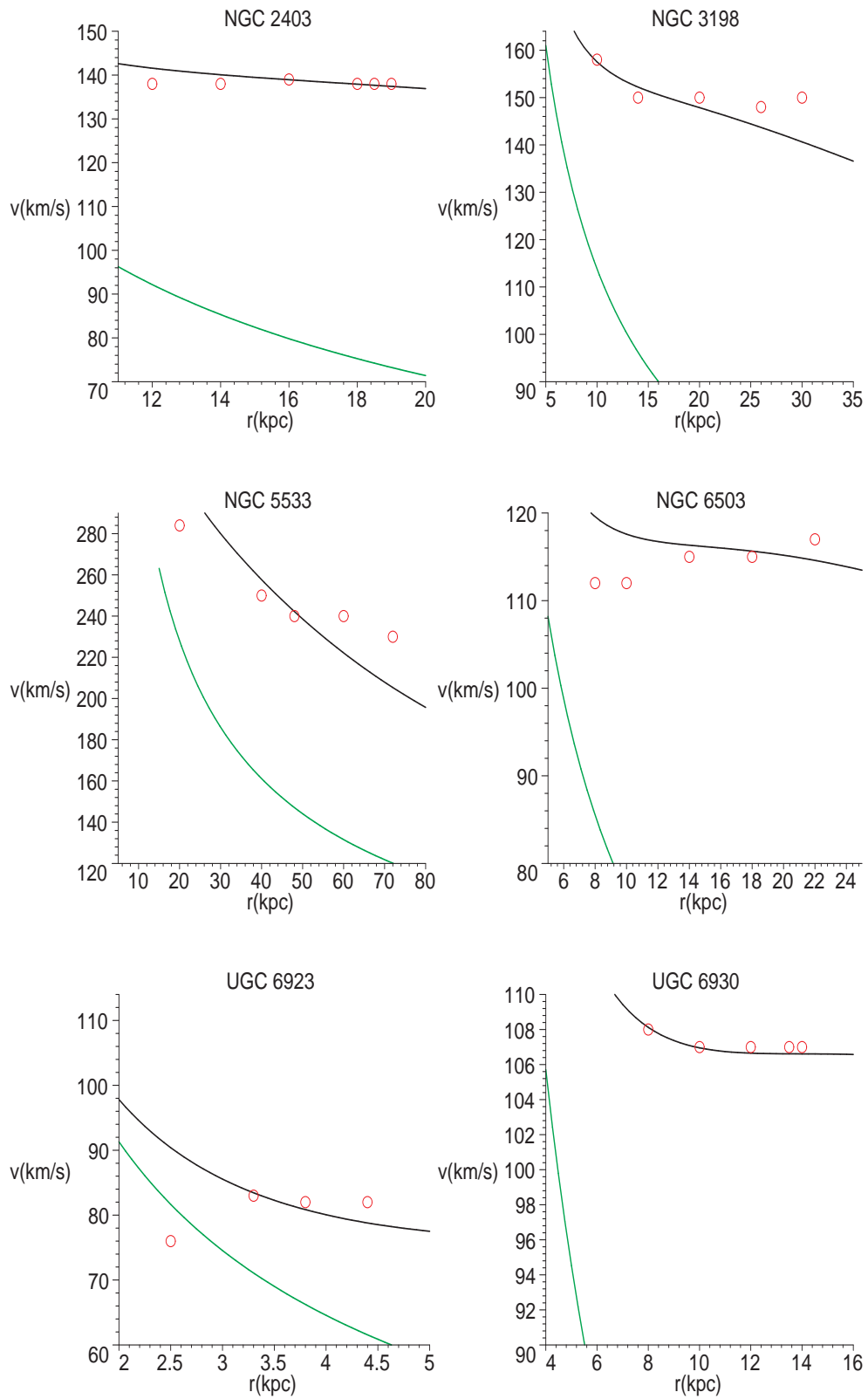
- [1] J. W. Moffat, gr-qc/0404076; astro-ph/0403266.
- [2] J. W. Moffat, Phys. Rev. **19**, 3554 (1979).
- [3] J. W. Moffat, Phys. Letts. **B 335**, 447 (1995), gr-qc/9411006.
- [4] J. W. Moffat, J. Math. Phys. **36**, 3722 (1995); Erratum, J. Math. Phys. **36**, 7128 (1995).
- [5] S. Perlmutter et al. *Astrophys. J.* **483**, 565 (1997), astro-ph/9608192; A. G. Riess, et al., *Astron. J.* **116**, 1009 (1998), astro-ph/9805201; P. M. Garnavich, et al. *Astrophys. J.* **509**, 74 (1998), astro-ph/9806396.
- [6] A. G. Riess et al., *Astrophys. J.* **607**, 665 (2004), astro-ph/0402512.

- [7] D. N. Spergel et al., *Astrophys. J. Suppl.* **148**, 175 (2003), astro-ph/0302209; C. L. Bennett et al., *Ap. J. Suppl.* **148**, 1 (2003), astro-ph/0302207.
- [8] M. Reuter and H. Weyer, *JCAP* 0412 (2004) 001, hep-th/0410119; hep-th/0410117; *Phys. Rev.* **D69**, (2004), 104022, hep-th/0311196.
- [9] T. Damour, S. Deser and J. McCarthy, *Phys. Rev.* **D47**, 1541 (1993), gr-qc/9207003.
- [10] M. Kalb and P. Ramond, *Phys. Rev.* **D9**, 2273 (1974).
- [11] C. W. Stubbs et al. *Phys. Rev. Lett.* **58**, 1070 (1987); E. G. Adelberger et al. *Phys. Rev. Lett.* **59**, 849 (1987); E. G. Adelberger, et al. *Phys. Rev.* **D42**, 3267 (1990).
- [12] J. W. Moffat and I. Yu. Sokolov, *Phys. Lett.* **B378**, 59 (1996), astro-ph/9509143.
- [13] <http://pdg.lbl.gov>.
- [14] R. H. Sanders and S. S. McGaugh, *Ann. Rev. Astron. Astrophys.* **40**, 263 (2002), astro-ph/0204521.
- [15] R. B. Tully and J. R. Fisher, *Astr. Ap.* **54**, 661 (1977).
- [16] E. L. Lokas, *Mon. Not. R. Astron. Soc.* **333**, 697 (2002), astro-ph/0112023.
- [17] M. Mateo, *Ann. Rev. Astron. Astrophys.* **36**, 435 (1998).
- [18] J. Kormendy and K. C. Freeman, *Dark Matter in Galaxies*, Proceedings of the IAU Symposium No. 220, 2004 IAU, eds. S. Ryder, D. J. Pisano, M. Walker and K. C. Freedman, San Francisco: ASP, 2004, astro-ph/0407321.
- [19] A. J. Romanowsky et al., *Science Express Reports*, 28 August, 2003, astro-ph/0308518; A. J. Romanowsky et al. *Dark matter in Galaxies*, Proc. IAU Symposium No. 220, eds. S. Ryder, D. J. Pisano, M. Walker and K. Freedman, San Francisco: ASP, 2004, astro-ph/0310874.
- [20] M. Milgrom, *Astrophys. J.* **270**, 365 (1983).
- [21] J. D. Bekenstein, *Phys. Rev.* **D70** (2004) 083509, astro-ph/0403694.
- [22] M. Milgrom and R. H. Sanders, *Astrophys. J.* **599**, L25 (2003), astro-ph/0309617.
- [23] D. E. McLaughlin and G. Meylan, *New Horizons in Globular Cluster Astronomy* ASP Conference Series, 2003, eds. G. Piotto, G. Meylan, G. Djorgovski and M. Riello.

- [24] K. G. Begeman, A. H. Broeils and R. H. Sanders, *Mon. Not. R. Astr. Soc.* **249**, 523 (1991).
- [25] Y. Sofue et al., *Astrophys. J.* **523**, 136 (1999).
- [26] F. Prada et al., *Astrophys. J.* **598**, 260 (2003), astro-ph/0301360.
- [27] V. Avila-Rees et al., *Astrophys. J.* **559**, 516 (2001), astro-ph/0010525; P. Colin et al., *Astrophys. J.* **581**, 777 (2002), astro-ph/0205322.
- [28] J. D. Bekenstein and R. H. Sanders, *Astrophys. J.* **429**, 480 (1994), astro-ph/9311062.
- [29] R. D. Blanford and R. Narayan, *Ann. Rev. Astron. Astrophys.* **30**, 311 1992.
- [30] M. Reuter and H. Weyer, hep-th/0410117; hep-th/04101179.
- [31] M. Reuter, *Phys. Rev.* **D57**, 971 (1998), hep-th/9605030.
- [32] I. L. Shapiro, J. Sola and H. Stefancic, hep-ph/0410095.
- [33] S. Weinberg in *General Relativity, an Einstein Centenary Survey*, S. W. Hawking and W. Israel (Eds.), Cambridge University Press (1979); S. Weinberg, hep-th/9702027.
- [34] O. Lauscher and M. Reuter, *Phys. Rev.* **D65**, (2002) 025013, hep-th/0108040.
- [35] W. Souma, *Prog. Theor. Phys.* **102**, 181 (1999), hep-th/9907027.
- [36] R. Percacci and D. Perini, *Phys. Rev.* **D67**, 081503 (R) (2002), hep-th/0207033; hep-th/0401071.
- [37] S. Burles, K. M. Nollett and M. S. Turner, *Phys. Rev.* **D63** (2001) 063512, astro-ph/0008495.
- [38] J. G. Williams, S. G. Turyshev and D. H. Boggs, gr-qc/0411113.
- [39] L. Wang, R. R. Caldwell, J. P. Ostriker, P. J. Steinhardt, *Astrophys. J.* **530**, 17 (2000), astro-ph/9901388.
- [40] A more extensive fit to the galaxy data using a least squares fitting routine will be presented elsewhere: J. R. Brownstein and J. W. Moffat, in preparation.

Table 1. Values of the total galaxy mass M used to fit rotational velocity data. Also shown are the mass-to-light-ratios M/L with L obtained from ref. [14].

Galaxy	$M(\times 10^{10} M_{\odot})$	$M/L(M_{\odot}/L_{\odot})$
NGC 5533	24.2	4.29
NGC 5907	11.8	4.92
NGC 6503	1.36	2.84
NGC 3198	3.0	3.33
NGC 2403	2.37	3.0
NGC 4138	2.94	3.59
NGC 3379	5.78	—
M33	0.93	1.98
UGC 6917	0.96	2.53
UGC 6923	0.388	1.76
UGC 6930	1.04	2.08
FORNAX	0.0026	1.86
DRACO	0.00050	27.94
ω Centauri	3.05×10^{-5}	—



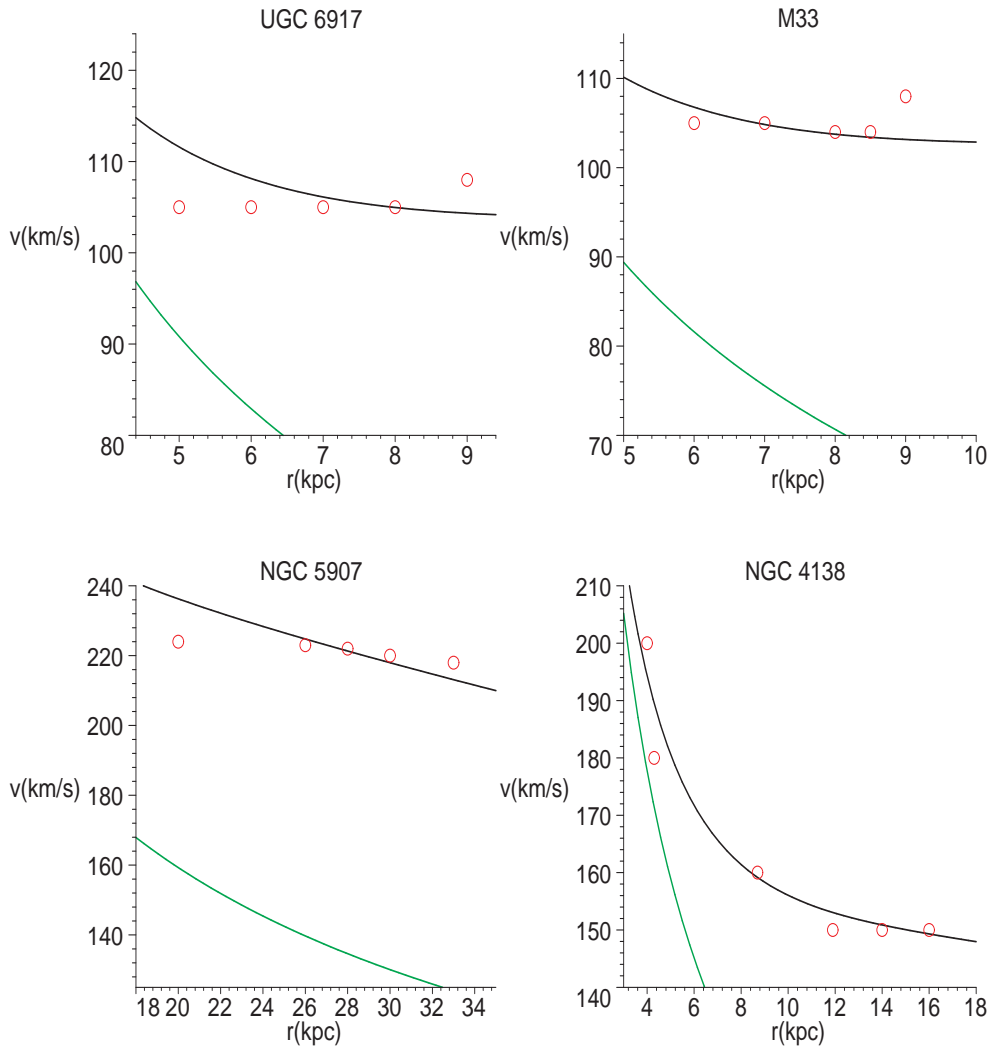


Fig. 1 - Fits to low-surface-brightness and high-surface-brightness spiral galaxy data. The black curve is the rotational velocity v versus r obtained from the modified Newtonian acceleration, while the green curve shows the Newtonian rotational velocity v versus r . The data are shown as red circles.

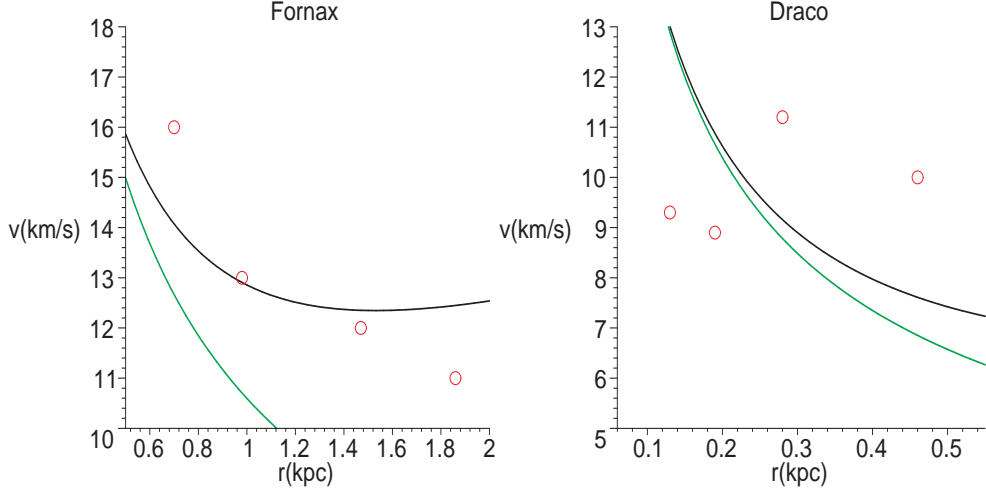


Fig. 2 - Fits to the data of two dwarf galaxies Fornax and Draco. The simple relation $V \sim \sqrt{2}\sigma$ is assumed between the velocity dispersion σ and the rotational velocity v . The black curve is the rotational velocity v versus r obtained from the modified Newtonian acceleration, while the green curve shows the Newtonian rotational velocity v versus r . The data are shown as red circles and the errors (not shown) are large and for Draco the Newtonian fit cannot be distinguished from the MSTG fit to the data within the errors.

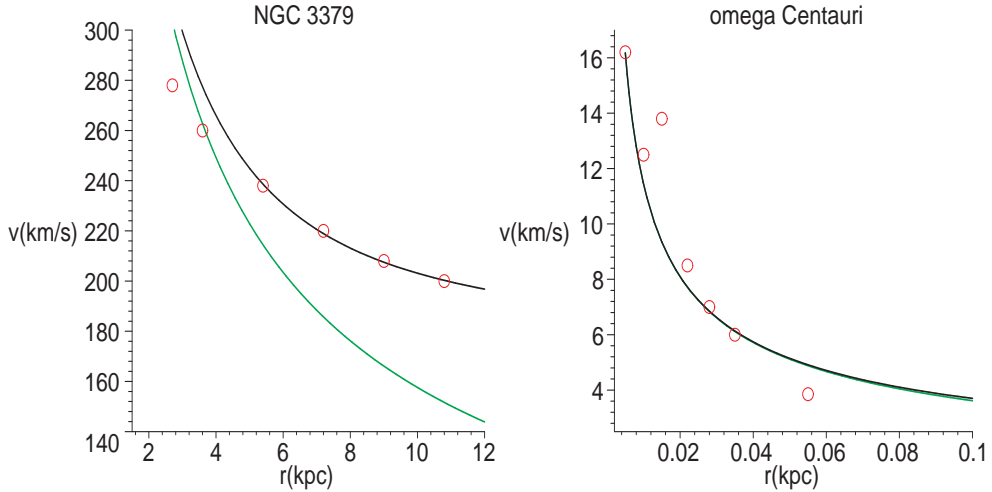


Fig. 3 - Fits to the elliptical galaxy NGC 3379 and the globular cluster ω Centauri. The black curve is the rotational velocity v versus r obtained from the modified MSTG acceleration, while the green curve is the Newtonian-Kepler velocity curve. For ω Centauri the black and green curves cannot be distinguished from one another.

Fig. 4 - Fits to the rotation curves for the four galaxies NGC 1560, NGC 2903, NGC 4565 and NGC 5055. The black curve is the rotational velocity v versus r obtained from the modified MSTG acceleration formula (59), while the green curve is the Newtonian-Kepler velocity curve for the core-Newtonian acceleration formula (63). The luminous mass used to fit the data for NGC 1560 is $M = 1.51 \times 10^{10} M_{\odot}$, while the core radius is $r_c = 1.5 \times 10^{22} \text{ cm} = 4.85 \text{ kpc}$. For NGC 2903 the luminous mass used to fit the data is $M = 9.95 \times 10^{10} M_{\odot}$, while the core radius is $r_c = 2.75 \text{ kpc}$. For NGC 4565 the luminous mass is $M = 1.81 \times 10^{11} M_{\odot}$, while the core radius is $r_c = 3.11 \text{ kpc}$. For NGC 5055 the luminous mass is $M = 8.55 \times 10^{10} M_{\odot}$ and the core radius is $r_c = 2.04 \text{ kpc}$.

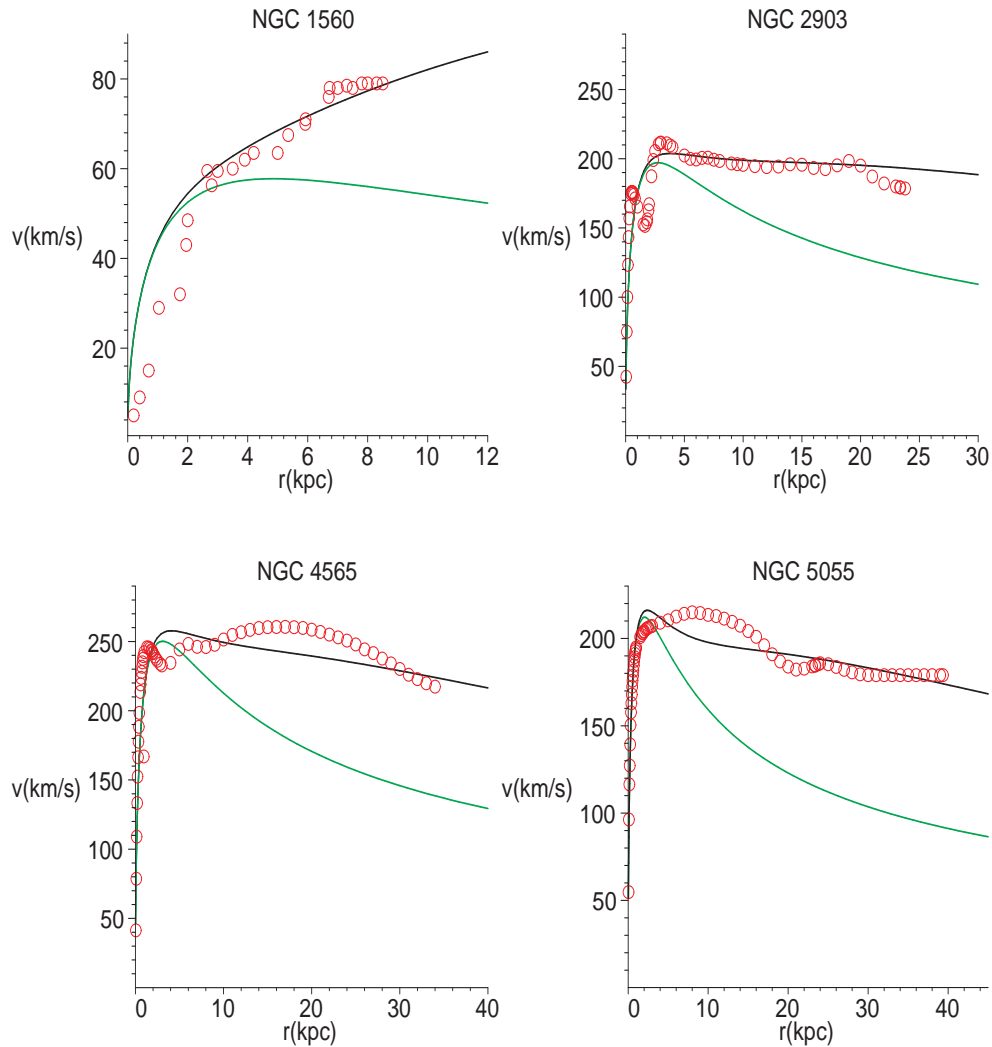


Fig. 5 - 3-dimensional plot of v versus the range of distance $0.1 \text{ kpc} < r < 10 \text{ kpc}$ and the range of galaxy mass $5 \times 10^6 M_\odot < M < 2.5 \times 10^{11} M_\odot$. The red surface shows the Newtonian values of the rotational velocity v , while the dark surface displays the MSTG prediction for v .

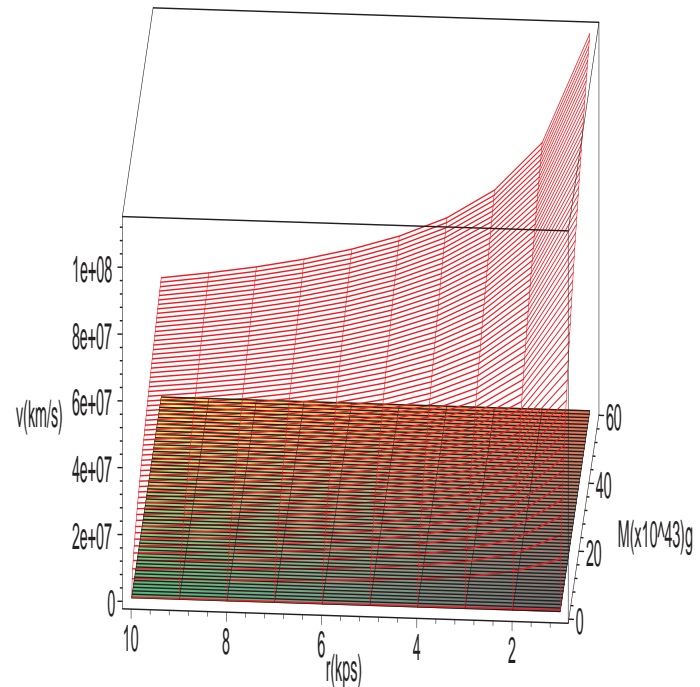


Fig. 6 - Plot of conjectured running of the effective gravitational constant $G(t)$ with time t .

